Dynamical fluctuations in In nanowires on Si(111)

Shinichiro Hatta, Yoshiyuki Ohtsubo, and Tetsuya Aruga
Department of Chemistry, Kyoto University and JST CREST, Kyoto 606-8502 Japan

Sanae Miyamoto and Hiroshi Okuyama
Department of Chemistry, Kyoto University, Kyoto 606-8502, Japan

Hiroo Tajiri and Osami Sakata
Research and Utilization Division, Japan Synchrotron Radiation Research Institute, SPring-8, Hyogo 679-5198, Japan

Temperature dependence of x-ray-diffraction profiles were measured during the disputed phase transition of the quasi-one-dimensional metallic nanowire system, In/Si(111). The diffraction intensity due to the interchain coupling showed a rapid decrease with increasing temperature from 115 to 125 K. In this temperature range, no significant broadening or diffuse scattering that should result from the fluctuation in the interchain order was observed. The intrachain structure factor, on the other hand, showed an increase as expected for the lifting of the Peierls distortion of the chains. We show that the present result is not well described by the order-disorder scenario. A pseudo-first-order transition mechanism is proposed as an alternative scenario based on the recent theoretical and experimental results.

I. INTRODUCTION

As a prototype of quantum nanowires, an array of indium atomic chains on Si(111) surface has been extensively studied during the past decade.[1] The system exhibits a metal-insulator transition at 120 K.[2–4] The driving mechanism was first proposed to be a weak-coupling Peierls instability. While further studies indicated an order-parameter fluctuation near T_c,[5–7] mechanisms based on the Peierls-type Fermi-surface nesting for the stabilization of the low-temperature (LT) phase appear to be consistent with a variety of experimental results. In the context of the Peierls-type continuous transition, the observed fluctuation may be understood as those inherent to low-dimensional systems.[8] On the other hand, an alternative scenario was proposed based on a molecular-dynamics (MD) simulation, in which it was suggested that the transition at 120 K is essentially an order-disorder type and the Peierls gap is maintained even at temperatures much higher than T_c.[9,10] This scenario corresponds to a strong-coupling regime of the Peierls-type charge-density wave (CDW) transitions,[11–13] in which a lattice-entropy-driven order-disorder transition proceeds at a temperature significantly lower than that for the electronic transition between the states with gapped and ungapped energy bands. The nature and extent of the fluctuation in the high-temperature (HT) phase has great implications for the physical properties of recent interests such as non-Fermi liquidity[14,15] and the quantum transport.[16,17] Thus the fluctuation effect in this system should be examined quantitatively.

For the structural phase transitions in bulk materials, intense research on the microscopic mechanism has been made since around 1960. In the so-called "soft-mode" model,[18,19] which shares many features with the Peierls-type CDW transitions, it was postulated that a particular phonon mode was softened with decreasing temperature and eventually frozen in at T_c to give rise to a static lattice displacement pattern. It turned out that the model was applicable only to a limited number of systems. On the other hand, the theoretical description

for the systems with strongly anharmonic potentials was developed,[20] which yielded a "domain-wall" solution that was adequate to the experimental observations for some phase transitions. Upon the excitation of domain walls, the system is characterized by the coexistence of two phases, thus the properties of the system are similar to those of a system undergoing a first-order transition. As far as we are aware, such a first-order-like mechanism has not been very extensively examined for the surface phase transitions, with a few exceptions.[7,21]

The Si(111) surface covered with 1 monolayer (ML) of In exhibits a sharp (4 × 1) diffraction pattern at room temperature, where 1 ML is defined as the atom density of Si(111). The structure model shown in Fig. 1(a), which consists of one-dimensional (1D) double In chains running parallel to [$\bar{1}$10], was found to be in good agreement with surface x-ray diffraction (SXRD).[22] The surface exhibits three nearly parabolic surface-state bands (m_1, m_2, and m_3) within projected bulk band gap, giving rise to quasi-1D Fermi contours.[2] The band structure is well reproduced by first-principles calculations based on the above structure model.[23]

As to the LT structure, most first-principles calculations suggested the Peierls-type pairing of the outermost atoms in the zigzag subchains and the formation of trimers, which induces a local (4 × 2) structure as shown in Fig. 1(b). The pairing causes gap formation at $\bar{X}'$ in two of the surface bands (m_2 and m_3) but leaves the other (m_1) metallic, which disagrees with semiconducting electronic structure observed by angle-resolved photoelectron spectroscopy (ARPES),[2,4,24] scanning tunneling spectroscopy (STS)[10] and transport experiments[17]. The discrepancy was resolved by González *et al.*,[9,25] who showed that shear deformation of the Peierls-distorted subchains to opposite directions, which yields "hexagons", forces an m_1-band electron pocket at $\bar{\Gamma}$ to shift above the Fermi level (E_F) and makes the surface insulating. This model was further supported by a scanning tunneling microscopy (STM) image simulation.[10]
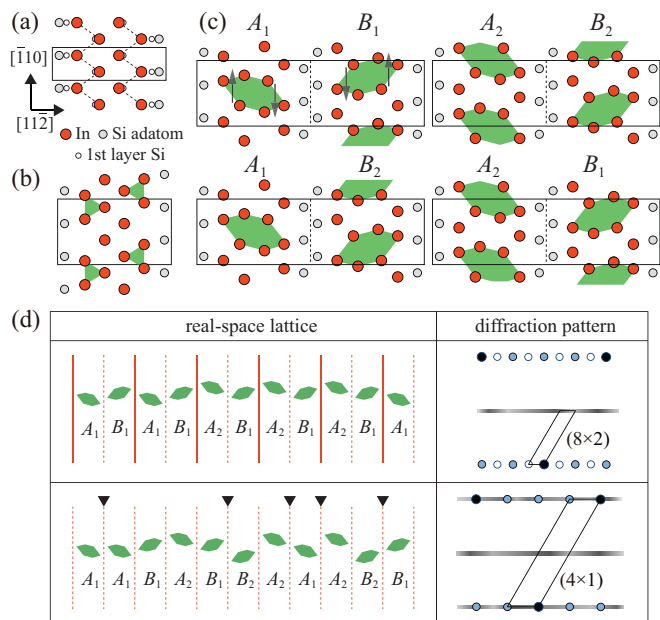
FIG. 1. (Color online) Models for (a) (4×1) and (b) trimer (4×2) structures. (c) Possible arrangements of (8×2) hexagon model. The arrows indicate shear displacement vectors. (d) Arrangements and diffraction patterns for $(8 \times$ "2") (upper panels) and dynamically fluctuating (4×2) chains (lower panel). Phase defects are indicated by triangles.

The hexagon model is shown in Fig. 1(c). There are two energetically equivalent (4×2) chain structures, here labeled A and B. Interchain coupling forces the A and B chains to order alternatively $(ABAB \ldots)$, resulting in an (8×2) unit cell. In addition, there is a phase degree of freedom along the chain, which is here denoted by a subscript $i = 1,2$. As a result, there are four symmetrically inequivalent (8×2) unit structures as shown in Fig. 1(c). Note that these four sublattices are energetically equivalent. Hence structures $A_i B_j (i, j = 1,2)$ are randomly intermixed in the actual surface as shown in the upper panel in Fig. 1(d). As a result the diffraction pattern of the LT phase gives rise to streaks along h at $k = n/2$ $(n \neq 0)$ [Figs. 2(a) and 2(b)]. The sharp 1/8-order diffraction spots in Fig. 2(a) indicate that the alternative $ABAB \ldots$ arrangement is ordered in a long range. The symmetry of the actual LT structure is denoted as $(8 \times$ "2"). Previous LEED observations indicated that the long-range $\times 8$ and $\times 2$ orders disappear concomitantly.[7,26]

In the order-disorder scenario,[9,10] it is argued that the system fluctuates dynamically between degenerate ground states, which should give rise to an "average" (4×1) structure above T_c. The MD simulation employing a (4×2) unit cell showed that the Peierls distortion, and hence the Peierls gap at $\bar{X}'$, are maintained at temperatures higher than 200 K. It also showed that, due to the thermal excitation of shear phonon modes, the system temporarily visited the state with a trimerlike structure giving rise to a finite density of states at E_F (pseudogap) at $\bar{\Gamma}$. The result was supported for temperatures close to T_c by the weak metallicity observed by STS at 120 K.[10]

The order-disorder transition from the LT $(8 \times$ "2") to the average (4×1) surface should necessarily be associated with
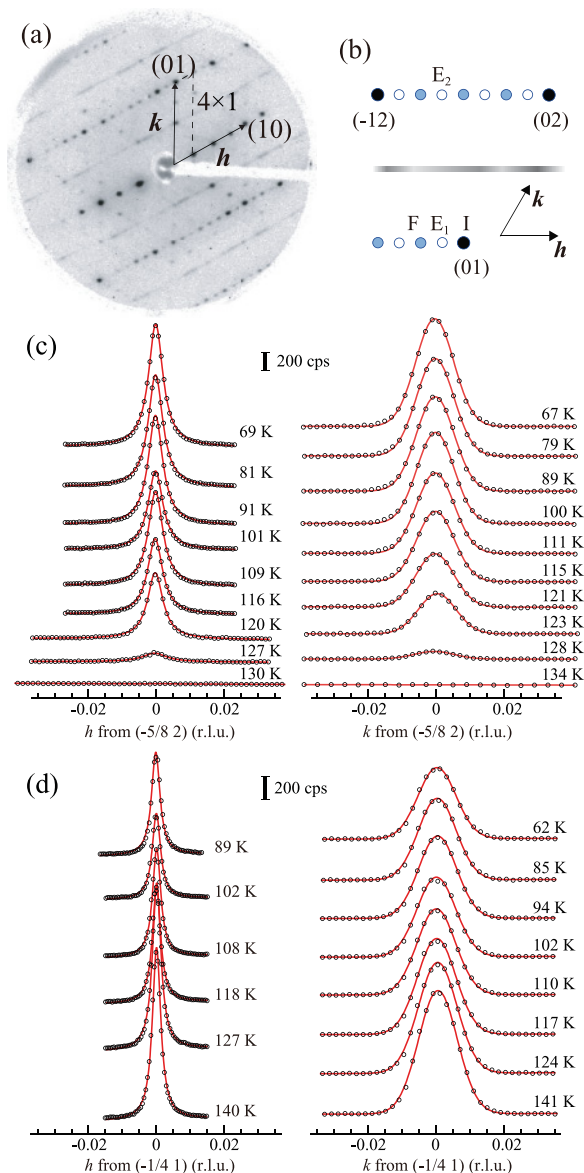
FIG. 2. (Color online) (a) A LEED pattern of In/Si(111)-$(8 \times$ "2") surface taken with 90-eV electrons at 47 K. (b) Schematic of the LT-phase LEED pattern. The spots measured by SXRD are indicated by alphabets: I (0 1), F $(-\frac{1}{4} 1)$, E_1 $(-\frac{1}{8} 1)$, E_2 $(-\frac{5}{8} 2)$. Measured line profiles at (c)1/8-order (E_2) and (d) 1/4-order (F) positions along h (left panels) and k (right panels). Intensities are normalized by the incident x-ray intensity (I_0) measured with an ion chamber. Solid lines represent Lorentzian (h scans) or Gaussian (k scans) curves fitted to the profiles.

the interconversion of A and B orientations. This should reduce the correlation length of the interchain order, resulting in critical scattering (streaks along h) at the 1/8-order diffraction spots. In the present work, we have examined the temperature dependence, in a range of 55–145 K, of diffraction intensities and profiles during the $(8 \times$ "2")–(4×1) transition by SXRD, which should provide a direct insight into the nature and extent of the fluctuation and serves as a critical test of the validity of the order-disorder scenario. In Sec. III A, we describe the experimental results in detail. In Secs. III A and III B, we will examine the order-disorder and the pseudo-first-order

scenarios, respectively, based on the present results as well as available results of recent theoretical and experimental works.

II. EXPERIMENT

The experiments were performed in an ultrahigh vacuum chamber mounted on a (2+2)-type diffractometer[27] at BL13XU of SPring-8.[28] The x-ray wavelength of 1.36 Å (9.1 keV) and the incident grazing angle of 1.0° were used. The reciprocal-lattice coordinates are here given by the low-energy electron-diffraction (LEED) convention, where a unit cell is defined by $\mathbf{a} = \frac{1}{2}[10\bar{1}]_{cubic}$, $\mathbf{b} = \frac{1}{2}[\bar{1}10]_{cubic}$, and $\mathbf{c} = [111]_{cubic}$. Line profiles are measured along the h direction ($[11\bar{2}]$, perpendicular to the In chain) and along k ($[\bar{1}10]$) at $l = 0.3$ reciprocal-lattice units (r.l.u.).

The sample of 30×7 mm^2 was cut from a nominally flat Si(111) wafer. Sharp triple-domain (7 × 7) LEED patterns were observed after flashing at ~1200 K several times. Indium was evaporated from an alumina crucible on the sample kept at 700 K by passing a dc current, which yielded a nearly single-domain (8ט2") LEED pattern as shown in Fig. 2(a) after cooling down to ⩽120 K. Sample temperature was monitored with a thermocouple welded to a Mo baseplate. Temperature dependence was measured with the sample temperature increasing slowly after the closed-cycle refrigerator was turned off.[29] The change of the z coordinate (~1 μm/min) due to gradual elongation of the manipulator

rod upon temperature rise was monitored and compensated for every scan.

III. RESULTS AND DISCUSSION

A. Temperature dependence of the diffraction profiles

Figures 2(c) and 2(d) show the line profiles of the 1/8-order [E$_2$ in Fig. 2(b)] and 1/4-order (F) diffraction spots upon elevating temperature. The profiles along h and k are well fitted with Lorentzian and Gaussian curves, respectively. Traveling along h is achieved mainly by the sample rotation about the surface normal, giving rise to a high-resolution profile. The k scan is associated with the rotation of other axes, unavoidably associated with a broader instrumental function corresponding to a transfer width ~260 Å. Note that the sharp Lorentzian line shape at low temperatures of E$_2$ along h evidences the long-range $ABAB\ldots$ order.

The peak heights as a function of temperature are shown in Fig. 3(a). The labels E$_1(k)$, etc., denote the k scan for the E$_1$ spot and so on. The height of the integer-order spot increases gradually by ~25% from 55 to 140 K. This intensity increase is due to the x-ray reflectivity change associated with the change of the incidence angle by ~0.05°, which is induced by nonaxial distortion of the manipulator rod upon temperature rise. Note that the sample tilting by ~0.05° induces the change of the in-plane reciprocal coordinates ($\delta h, \delta k \leqslant 5 \times 10^{-5}$ r.l.u.), which, however, is negligible as compared with the width
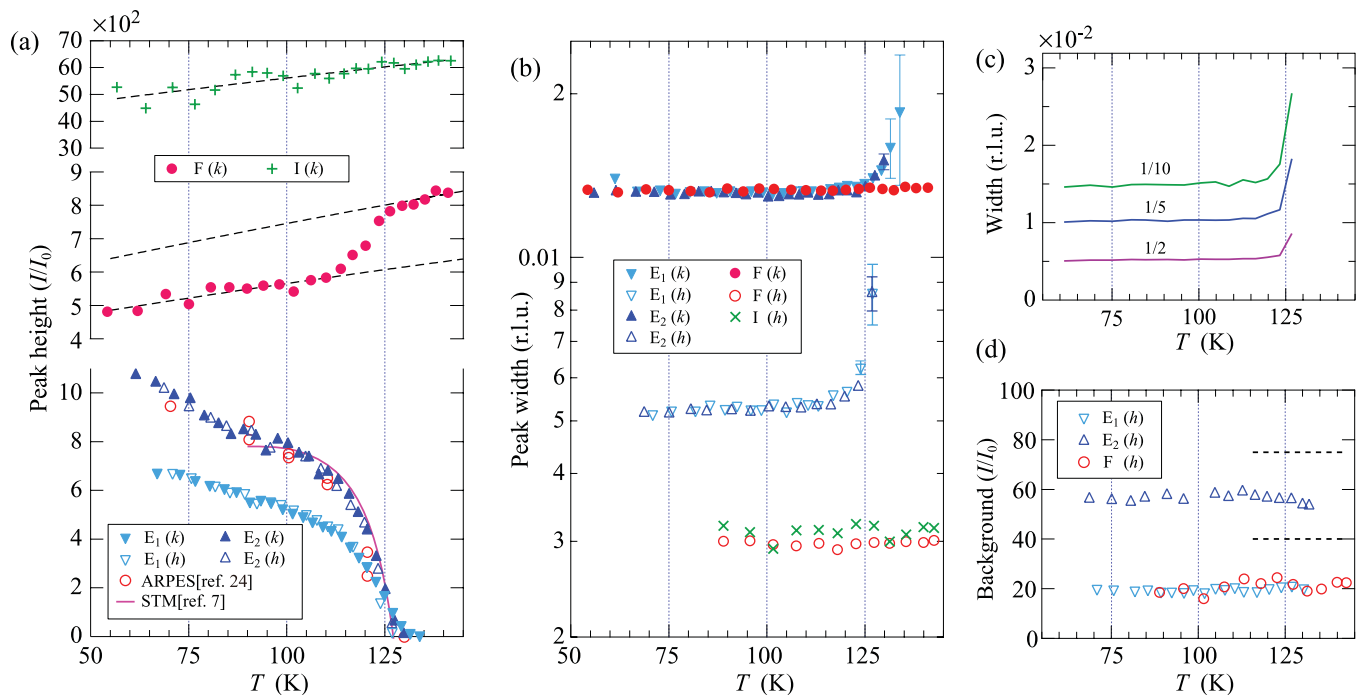
FIG. 3. (Color online) (a) The peak heights normalized to the instrumental functions for the integer (I), 1/4-order (F), and 1/8-order (E$_1$ and E$_2$) spots as a function of temperature. The labels E$_1(k)$, etc. denote the k scan for the E$_1$ spot, and so on. Broken lines shown with the integer- and 1/4-order intensities indicate the intensity variation due to the reflectivity change and the Debye-Waller factor (see text). The 1/8-order intensity is normalized to this intensity variation. Along with the 1/8-order intensity, partial intensity of the LT-phase band measured by ARPES (Ref. 24) is shown by open circles, and spatial occupation ratio of the insulating domain observed by STM (Ref. 7) are shown by the solid line. (b) The widths of I, F, E$_1$, E$_2$ along h and k as a function of temperature. (c) The widths of E$_2$ along h measured at the half (low), one-fifth (middle), and one-tenth (high) of maxima for the h scan. (d) Background intensities determined for the h scans of the 1/8- (E$_1$, E$_2$) and 1/4-order (F) spots. Dashed lines indicate the calculated intensity of the streaks for the randomly fluctuating (4 × 2) chains.

of the diffraction profiles. While the change in out-of-plane coordinate might be larger ($\delta l \leqslant 5 \times 10^{-4}$ r.l.u.), this also is negligible because the intensity variation along l is very moderate for surface reciprocal rods as well as for crystal truncation rods at $l = 0.3$.

The reflectivity change should also affect on the intensities of the fractional-order spots. In Fig. 3(a), the variation of the integer-order spot intensity is shown by broken lines along with the raw intensities of the 1/4-order spot, F. Note that the intensity variation due to the Debye-Waller factor is included in the curve. The intensity change of F below 115 K and above 125 K agrees with that of the integer order spot indicated by the broken lines, indicating no significant change in the 1/4-order structure. In the temperature range 115–125 K, the 1/4-order intensity increases by ∼30%. The increase implies the structural change within the (4×2) unit cell. We calculated the difference in diffraction intensity of the $(-\frac{1}{4}\ 1)$ spot for the structure models obtained by first-principles calculation,[9] which showed that the intensity from undistorted (4×1) is larger by 41% than that from hexagon (4×2), in reasonable agreement with the observed change.

The heights of the 1/8-order spots E_1 and E_2 reduce gradually by ∼40% with increasing temperature from 60 to ∼115 K, and more rapidly from 115 to 130 K, where the intensity increase of the 1/4-order spot was observed. The spots are under the detection limit ($I/I_0 < 5$), which is defined by the noise level, at $T \geqslant 130$ K. Note that the 1/8-order intensity is normalized to that of the integer-order spot.

The peak widths measured at half maxima along h and k as a function of temperature are shown in Fig. 3(b). At lower temperatures, the widths are constant at 0.003 r.l.u. (integer and 1/4 order) and 0.005 r.l.u. (1/8 order) along h, which corresponds to correlation lengths of 1100 and 700 Å, respectively. The shorter 1/8-order correlation length indicates that a small amount of phase defects such as $\ldots ABAABA \ldots$ and $\ldots BABBAB \ldots$ are formed intrinsically in the $(8 \times$ "2") phase.

With increasing temperature, the 1/8-order widths along h are almost constant up to 120 K, at which the intensity is reduced to ∼70% of that at 100 K. It is above ∼123 K that the 1/8-order spots are significantly broadened. The width along h increases to 0.009 r.l.u. at 127 K, above which the 1/8-order spots diminish. In order to examine whether there is a weak diffuse component, we compare the peak widths at half, one-fifth, and one-tenth of the maxima [Fig. 3(c)], which show no hint of a diffuse component below 115 K. The broadening above 123 K should be ascribed to the reduction of the correlation length of the $\times 8$ interchain order. The microscopic mechanism will be discussed below.

B. Order-disorder scenario

The Peierls-type CDW transitions can be classified according to the strength of the electronphonon coupling. In the weak-coupling regime, where the Peierls gap is very small (∼50 meV at most), the transition may be described by the mean-field theory and is expected to undergo continuous displacement of the atoms. In the strong-coupling regime,[11–13] characterized by a larger Peierls gap, the transition temperature expected from the mean-field theory, T_p, becomes higher than a few hundreds

of K. In such cases, the long-range order of the CDW state can easily be destroyed by the excitation of a phonon mode that is not relevant to the Peierls distortion at a temperature much lower than T_p, thus resulting in an order-disorder transition, thus giving rise to critical scattering. The mechanism of the strong-coupling CDW transitions has been well discussed, for example, for the (001) surfaces of W and Mo.[11,30,31]

In the scenario proposed by González and co-workers,[9,10] it was suggested that the shear phonon mode, which is not relevant to the Peierls distortion, is thermally excited at ∼120 K, resulting in the metallization of the m_3 band, while the $\times 2$ Peierls distortion is maintained up to much higher temperatures. Their scenario falls into the strong-coupling CDW regime.

In their MD simulation,[9,10] the (4×2) unit cell was employed, which means that all the double chains fluctuate among four possible structures (A_1, A_2, B_1, and B_2) with the spatial phase of each double chain synchronized. In the real $(8 \times$ "2") surface, however, the dynamical fluctuation should be associated with the destruction of the long-range interchain ($ABAB \ldots$) order; otherwise the $\times 8$ diffraction spots would not disappear upon the transition. The $\times 2$ long-range order along the chain direction also disappears at 125 K concomitantly with the $\times 8$ order.[7] Hence the dynamical fluctuation should also destroy the long-range intrachain order at the same temperature as that for the *interchain* order. The destruction of the intrachain order corresponds to the introduction of phase defects between A and B within each chain. Thus the anticipated order-disorder transition should belong to the two-dimensional (2D) Ising universality class. While the interaction in the directions parallel and perpendicular to the chains should be anisotropic, this does not affect on the critical behavior. Note that, while the spatial phase of each chain is disordered in the LT phase, the concomitant disappearance of the $\times$ "2" streaks and the $\times 8$ diffraction spots implies that the critical behavior is maintained in the temperature dependence of the $\times 8$ diffraction features. Since the $A_i B_j (i, j = 1,2)$ sublattices are energetically degenerate, the spatial phase degree of freedom of each chain should not play any significant role.

The critical scattering theory suggests that the long-range-order intensity I_{long}, the "susceptibility" χ, which corresponds to the intensity of the diffuse diffraction feature due to the short-range order, and the correlation length ξ of the short-range order are scaled to the power of the reduced temperature, $t = (T - T_c)/T_c$, as $I_{\text{long}} \propto (-t)^{2\beta}$, $\chi \propto |t|^{-\gamma}$, and $\xi \propto t^{-\nu}$. For the 2D Ising universality class, the critical exponents should be $\beta = 1/8$, $\gamma = 7/4$, and $\nu = 1$. Empirically, it is well established that the critical power-law behavior is observed within a range of about $|t| \leqslant 0.1$ (For a surface example, see Refs. 29 and 32–34). The temperature range of our data set corresponds to $-0.55 \leqslant t \leqslant 0.18$, which well covers the critical region.

In Fig. 4, the intensity of the 1/8-order spots, which represent I_{long} for $t \leqslant 0$ and χ for $t \geqslant 0$, and its width, which represents $1/\xi$ for $t \geqslant 0$, are plotted again. The width is constant at 0.0053 r.l.u. up to 115 K, implying that the long-range order is maintained up to 115 K. The width exhibits a slight increase above 115 K, and starts to increase more steeply above 123 K. This may suggest that T_c lies between

115 and 123 K. Note that the peak heights at 115 and 123 K are ~95% and ~45%, respectively, of that at 110 K, which appears to be unusual for the order-disorder transition since, in usual cases, the intensity decreases to 10–20% of that in the LT phase at T_c, at which the width starts to increase. In the present data, the diffraction spot is observed up to 127 K, which corresponds to $t = 0.06$ for $T_c = 120$ K, and is below the detection limit ($I/I_0 < 5$) at 130 K as shown in Fig. 4(d). This is unexpected for a usual order-disorder transition. For comparison, in the case of the 2D Ising transition on In/Cu(001), which was studied with a nearly identical experimental geometry at the same beamline, the critical scattering was observed up to $t \sim 0.25$.[29] For the four-state Potts model, which is the other universality class that gives a continuous transition at surfaces,[35] $\gamma = 7/6$ is expected, which would result in even more moderate attenuation of the critical scattering.[34]

We show in Fig. 4(a) the power-law functions fitted to the data with T_c assumed to be 117, 120.5, and 122 K. The exponents are fixed at the values for the 2D Ising class. For the fitting with $T_c = 117$ K, the peak width $1/\xi(t)$ is fitted properly for the data above 122 K, but the agreement is very poor for the peak height above T_c, $\chi(t)$. The experimental peak-height data in the range $\geqslant 120$ K varies convex upward, which is inconsistent with the expected function $\chi \propto t^{-\gamma}$. Thus the $T_c < 120$ K is highly improbable. For $T_c = 120.5$ K, the $\chi(t)$ curve shows a significant discrepancy with the data. The fitting of the $\chi(t)$ curve to the data at 123–127 K predicts the peak height of $I/I_0 \sim 30$ at 130 K, at which, however, the peak is below the detection limit. For $T_c = 122$ K, the agreement of $\chi(t)$ is even worse. In Fig. 4(b), we show the results of the fitting with the exponents fixed at $\nu = 2/3$ and $\gamma = 7/6$, which is expected for the four-state Potts model. The agreement is again very poor. We also fitted the power-law functions with the exponents treated as adjustable parameters [Fig. 4(c)]. The fitting of $1/\xi(t)$ yielded $\nu = 0.3$–0.5, which is much smaller than that expected for the 2D Ising model. The agreement of the fitting to $\chi(t)$ is very poor again; the intensity below the detection limit at 130 K is incompatible with the curves fitted to the data for lower temperatures.

Overall, we should conclude that the agreement of the experimental data with the critical scattering theory for the order-disorder transition is very poor. The most important problem is that the peak height is decreased very quickly above the temperature at which the broadening sets in, which is inconsistent with any universality class. As a result, the change in the peak width is observed only in a very limited temperature range, and hence the fitting to the peak width, which is usually more reliable in determining the universality class, does not serve any significant result. It should be concluded that the critical scattering, if any, associated with the phase transition studied in the present work is very weak as compared with the previously established order-disorder transitions at surfaces.

One may argue that the critical scattering might have been overlooked because the attenuation of $\chi(t)$ is unexpectedly steep for some reason. In order to address this possibility, we next discuss on the background intensity. Irrespective whether or not it belongs to any universality class, the dynamical fluctuation of the interchain order should give rise to streaks at $k = n$ along h [Fig. 1(d)] complementarily upon the decrease and disappearance of the 1/8-order diffraction intensity. As far
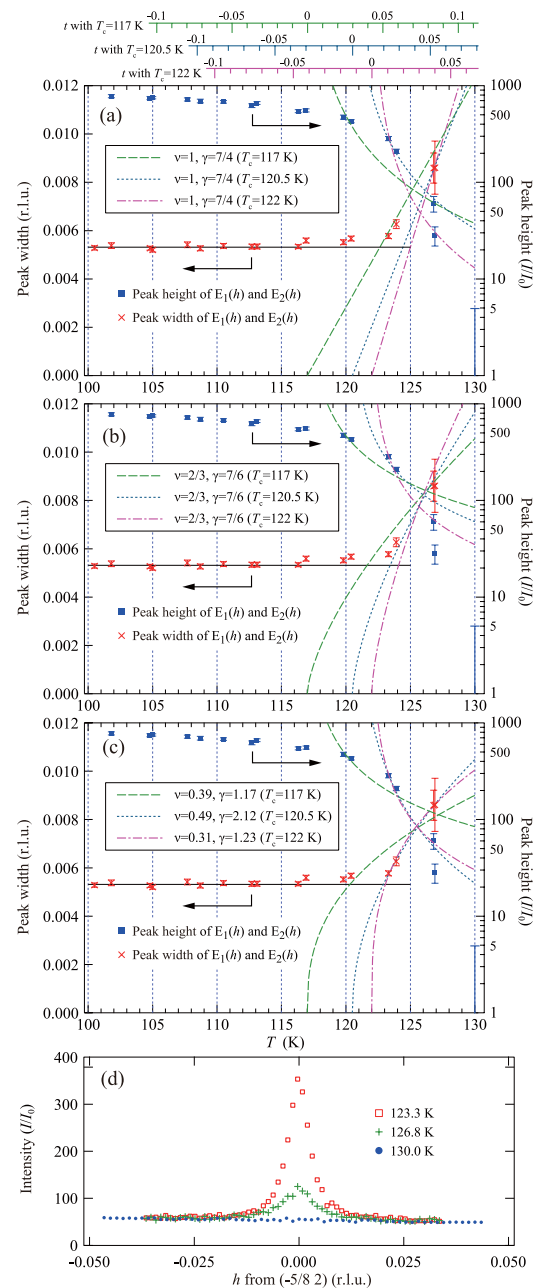
FIG. 4. (Color online) (a) The power-law curves fitted to the 1/8-order intensity and width data for $T > T_c$ with the exponents fixed at $\gamma = 7/4$ and $\nu = 1$ and T_c assumed to be 117 (broken curves), 120.5 (dotted curves), and 122 K (dot-dashed curves). (b) The same as (a) but with the exponents fixed at $\gamma = 7/6$ and $\nu = 2/3$. (c) The same as (a) but with the exponents treated as adjustable parameters. (d) Profiles of E_2 along h at increasing temperatures.

as we are aware, however, the streak at $k = n$ upon the phase transition has never been reported in the previous diffraction studies. In the present study, we examined the streaks at $k = n$ is observed by SXRD. The streaks can be directly monitored by the increase of the background intensity in the scans along h shown in the left panels in Figs. 2(c) and 2(d). Figure 3(d) shows the background intensities determined from the h scans along the line intersecting the 1/8- and 1/4-order spots. The background at temperatures lower than 100 K indicates the

level of the uniform 2D background. While the streak intensity is expected to be added to this level, no significant increase is observed.

In order to compare with the measured background, we calculated the background increase due to the streak. The intensities of the streaks and 1/4-order spots for completely disordered (4 × 2) chains were simulated. The absolute streak intensity was then determined by scaling the calculated 1/4-order intensities to the corresponding experimental data. Note that, if the correlation length along the chain direction is finite, the streaks would be broadened along the direction perpendicular to the streaks. Hence the correlation length along the chain direction was set at $30a$, where a is the surface lattice constant of Si(111), which is smaller than that deduced from the observed maximum width of the 1/8-order spots along k. This means that the simulation gives the lower limit of the streak intensity. The calculated streak intensity for completely disordered chains are shown by the dashed lines in Fig. 3(d). It is evident that there is no significant fluctuation in the interchain order in the temperature range 115–130 K where the 1/8-order structure factor decreases and diminishes. The result is in accordance with the very weak critical scattering.

We find further difficulty in interpreting the data in terms of the order-disorder scenario. As shown in Fig. 3(a), the intensity of the 1/4-order spot shows an increase at 115–125 K that is consistent with the structural change from (8 × "2") to (4 × 1). Note that this change was not reported in the molecular-dynamics simulation. Along the order-disorder scenario, one may argue that this structural change corresponds to the shift of the *average* atomic positions. However, as already discussed, T_c of the order-disorder transition cannot be lower than 120 K. Hence it should be argued that the dynamical fluctuation, if any, sets in at a temperature *higher* than the continuous structural transition. This picture contradicts the strong-coupling CDW theory, which predicts the order-disorder transition at a temperature *lower* than that for the relaxation of the Peierls distortion.

Thus we must conclude that, while there may be moderate phonon fluctuation, order-disorder processes should not be the dominant mechanism of the phase transition.

C. Pseudo-first-order scenario

As discussed in the previous subsection, the SXRD data do not indicate significant critical scattering. On the other hand, the relatively large fundamental energy gap of 0.1–0.3 eV of the LT phase[10,17] excludes the possibility of the (hypothetical) weak-coupling CDW transition, which means that the change of the 1/4- and 1/8-order structure factors in the 115–125-K range cannot be addressed to continuous and uniform displacement of the atomic positions.

Figure 5(a) shows the temperature dependence of the Landau-Ginzburg-like free-energy functional for a weak-coupling CDW transition as a function of the order parameter Δ, corresponding to a configurational coordinate of the system. Upon approaching T_c from below, the minimum of the free energy continuously shifts to $\Delta = 0$, which corresponds to a metallic phase, resulting in a second-order transition. This is essentially true for the cases that the free-energy functional do not have a local minimum at $\Delta = 0$. In the present
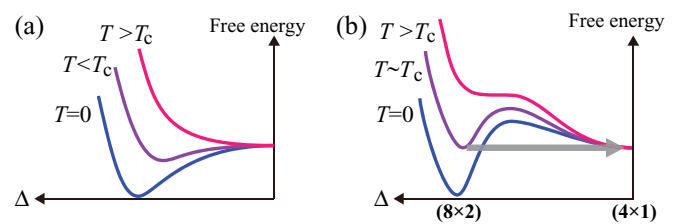
FIG. 5. (Color online) Schematic free-energy diagram for (a) a continuous transition expected for a weak-coupling 1D CDW and (b) continuous relaxation followed by a first-order transition.

system, however, the most recent first-principles total-energy calculation[16] indicates the existence of a local minimum at $\Delta = 0$, corresponding to the metallic (4 × 1) structure. As a result, the free-energy functional has a form typical of first-order transitions as schematically represented in Fig. 5(b). As the temperature increases from $T = 0$, the minimum is shifted gradually to smaller Δ to some extent. When the temperature approaches T_c, however, the first-order process sets in and the probability density is transferred from the minimum at (8 × 2) to that at (4 × 1).

In the phase transition with a first-order free-energy functional,[36,37] the critical fluctuation manifests itself predominantly as propagating nonlinear modes that serve as domain walls between coexisting phases.[38] The propagating domain walls cause the tunneling between two minima in the free-energy functional [Fig. 5(b)]. The domain-wall theory gave a good account of the features observed in many bulk transitions such as a large quasielastic intensity ("central peak") observed in the neutron-scattering spectra, the absence of significant critical scattering, precursor structures formed far above T_c, and a finite discontinuity in the microscopic order parameter.[20]

For the phase transition in the In chains on Si(111), no evidence for the finite discontinuity of the *average* order parameter has been observed in the present SXRD experiments, which implies that the transition does not belong to the first-order transition in thermodynamic definition. However, the present work shows that the structural change undergoes no significant lattice disordering. This strongly suggests that the critical behavior is not well described by dynamical phonon fluctuations as observed in the previous MD simulation with a minimal system size, but instead the domain walls play a major role as elementary excitation. The discontinuity in the average order parameter may be smeared by the finite-size effect[39] associated with a finite density of surface steps, quasi-one-dimensionality[40] or other microscopic reasons,[21] thus yielding a *pseudo*-first-order behavior. It should be noted that the term "pseudo-first-order behavior" is used here to emphasize that the microscopic mechanism is governed by propagating domain walls rather than soft phonons. We show below that the temperature-dependent behaviors of both the electronic and structural properties of this system are very similar to those of a system that undergoes a true first-order transition.

In their recent temperature-dependent ARPES study, Sun *et al.*[24] indicated that the well-defined HT and LT surface-state bands, which exhibited different dispersions not only near E_F but also down to 0.7 eV below E_F, coexisted in

a finite temperature range. Upon changing the temperature, the observed bands did not show continuous shift, but the spectral weights of the LT and HT bands changed in a complementary way. The totally different dispersion down to higher binding energies between the HT and LT phases rules out the weak-coupling Peierls model, which predicts only the change close to E_F. The partial intensity of the LT band measured by ARPES are shown by (red) open circles in Fig. 3(a), which is in good agreement with the 1/8-order SXRD intensity. It should be noticed that the increase of the 1/4-order SXRD intensity undergoes complementarily in the same temperature range. These indicate that the intensity change of both the 1/4- and 1/8-order spots are associated with the concomitant decrease and increase of the (8 × "2") and (4 × 1) domains, respectively, in a temperature interval of ∼20 K. It should be noted that the energy bands in the coexistence region are sharp. For instance, the width of the m_2 band for the metallic state, δk, at 120 K appears to be no larger than 0.05 Å^{-1} (Fig. 3 of Ref. 24), which suggests a large electronic coherence length ($2\pi/\delta k \sim 120$ Å) of the metallic phase even at 120 K.

The STM studies by different groups[5–7] indicated the coexistence of metallic and insulating phases at around the transition temperature. In the temperature-dependent STM observations, the fraction of insulating phase decreased steeply to nearly zero at T_c. We show in Fig. 3(a) the spatial occupation ratio of the insulating domain observed by STM[7] by a solid curve, which exhibits a good agreement with the 1/8-order SXRD intensity as well as the partial intensity of the LT-phase band measured by ARPES. Note that the agreement between the ARPES and STM data was pointed out previously.[24] Lee *et al.* argued that the nanoscale inhomogeneity similar to that observed by STM was also observed in the Monte Carlo simulation for the second-order transition.[6] We point out that, since phonons do not yield phase separation, the nanoscale phase coexistence should be a consequence of the excitation of domain walls. Proliferation of the nanoscale phase coexistence evidences that a pseudo-first-order mechanism dominates the system. The STM studies also indicated the formation of precursor patches of LT structure at temperature as high as 145 K,[6] which is often observed for first-order and pseudo-first-order transitions and explained in a natural way in terms of the nonlinear modes.[20]

The STM studies were sometimes criticized that the domains are pinned by local perturbations such as surface defects and tip effects. Indeed, the effect of surface defects has been acknowledged for the phase transition in the α phase of Sn and Pb on Ge(111).[41] It should be noted, however, that the significance of local perturbation is much different for each system. In the case of Sn(Pb)/Ge(111)-α, the electronic stabilization energy in the LT structure is gained over a wide area of surface Brillouin zone, resulting in a CDW correlation length as small as the unit-cell size. Due to narrow bandwidth

and a small group velocity near E_F, the system is very sensitive to local perturbations.[42] On the other hand, in the case of In/Si(111), the CDW correlation length estimated from the band-gap width is much larger (∼100 Å), and hence the system should be less sensitive to local perturbations.

Note that the domain size of the minority phase observed by STM in the phase coexistence region appears to be on the order of ∼10 chain widths,[5,7] which is close to the correlation length deduced from the width of the 1/8-order diffraction spots observed just before the extinction [Fig. 3(b)]. Therefore the slight broadening of the 1/8-order spots observed above 115 K would be ascribed, at least partly, to the decreasing size of the (8 × "2") domains during the pseudo-first-order transition process.

IV. CONCLUSION

In conclusion, we have studied the metal-insulator transition in In nanowires arrayed on Si(111) by SXRD. The result shows no significant 1D fluctuations of the interchain order upon the transition from the (8 × "2") to (4 × 1) phases. We also observed the increase of the 1/4-order structure factor concomitantly with the decrease of the 1/8-order structure factor. Since no finite discontinuity was observed, the transition is not classified to the first-order ones. Features such as (1) the lack of significant critical scattering, (2) no background increase in SXRD profiles, (3) the poor agreement of the temperature-dependent SXRD profiles with the critical scattering theory, and (4) the concomitant change of the LT and HT structure factors at temperatures lower than that for the peak broadening suggest that the order-disorder scenario is not applicable to the present system. We have proposed that the transition is essentially described in terms of a pseudo-first-order phase transition scenario, which is consistent with the above results (1)–(4) as well as (5) the first-order-type free-energy functional deduced from the first-principles calculation,[16] (6) the ARPES observation of the intensity switching between the well-defined LT and HT bands,[24] (7) the STM observations of domain structures during the transition,[5,7] and (8) the observation of a precursory structures at temperatures much higher than T_c.[5] Simulations devised to represent the present system would shed a further light on the critical behavior of this phase transition.

[1] P. C. Snijders and H. H. Weitering, Rev. Mod. Phys. **82**, 307 (2010).

[2] H. W. Yeom, S. Takeda, E. Rotenberg, I. Matsuda, K. Horikoshi, J. Schaefer, C. M. Lee, S. D. Kevan, T. Ohta, T. Nagao, and S. Hasegawa, Phys. Rev. Lett. **82**, 4898 (1999).

[3] S. J. Park, H. W. Yeom, S. H. Min, D. H. Park, and I.-W. Lyo, Phys. Rev. Lett. **93**, 106402 (2004).

[4] J. R. Ahn, J. H. Byun, H. Koh, E. Rotenberg, S. D. Kevan, and H. W. Yeom, Phys. Rev. Lett. **93**, 106401 (2004).

[5]J. Guo, G. Lee, and E. W. Plummer, Phys. Rev. Lett. **95**, 046102 (2005).

[6]G. Lee, J. Guo, and E. W. Plummer, Phys. Rev. Lett. **95**, 116103 (2005).

[7]S. J. Park, H. W. Yeom, J. R. Ahn, and I.-W. Lyo, Phys. Rev. Lett. **95**, 126102 (2005).

[8]G. Grüner, *Density Waves in Solids* (Addison-Wesley, Reading, MA, 1994).

[9]C. González, F. Flores, and J. Ortega, Phys. Rev. Lett. **96**, 136101 (2006).

[10]C. González, J. Guo, J. Ortega, F. Flores, and H. H. Weitering, Phys. Rev. Lett. **102**, 115501 (2009).

[11]T. Aruga, Surf. Sci. Rep. **61**, 283 (2006).

[12]W. L. McMillan, Phys. Rev. B **16**, 643 (1977).

[13]E. Tosatti, *Electronic Surface and Interface States on Metallic Systems*, edited by E. Bertel and M. Donath (World Scientific, Singapore, 1995), p. 67.

[14]C. G. Hwang, N. D. Kim, S. Y. Shin, and J. W. Chung, New J. Phys. **9**, 249 (2007).

[15]C. Liu, T. Inaoka, S. Yaginuma, T. Nakayama, M. Aono, and T. Nagao, Phys. Rev. B **77**, 205415 (2008).

[16]A. A. Stekolnikov, K. Seino, F. Bechstedt, S. Wippermann, W. G. Schmidt, A. Calzolari, and M. Buongiorno Nardelli, Phys. Rev. Lett. **98**, 026105 (2007).

[17]T. Tanikawa, I. Matsuda, T. Kanagawa, and S. Hasegawa, Phys. Rev. Lett. **93**, 016801 (2004).

[18]W. Cochran, Adv. Phys. **9**, 387 (1960).

[19]P. W. Anderson, *Fizika Dielectrikov*, edited by G. I. Skanavi (Acad. Nauk SSR, Moscow, 1960).

[20]J. A. Krumhansl and R. J. Gooding, Phys. Rev. B **39**, 3047 (1989).

[21]T. Nakagawa, O. Ohgami, Y. Saito, H. Okuyama, M. Nishijima, and T. Aruga, Phys. Rev. B **75**, 155409 (2007).

[22]O. Bunk, G. Falkenberg, J. H. Zeysing, L. Lottermoser, R. L. Johnson, M. Nielsen, F. Berg-Rasmussen, J. Baker, and R. Feidenhans'l, Phys. Rev. B **59**, 12228 (1999).

[23]J. H. Cho, D. H. Oh, K. S. Kim, and L. Kleinman, Phys. Rev. B **64**, 235302 (2001).

[24]Y. J. Sun, S. Agario, S. Souma, K. Sugawara, Y. Tago, T. Sato, and T. Takahashi, Phys. Rev. B **77**, 125115 (2008).

[25]C. González, J. Ortega, and F. Flores, New J. Phys. **7**, 100 (2005).

[26]S. Mizuno, Y. O. Mizuno, and H. Tochihara, Phys. Rev. B **67**, 195410 (2003).

[27]K. W. Evans-Lutterodt and Mau-Tsu Tang, J. Appl. Crystallogr. **28**, 318 (1995).

[28]O. Sakata, Y. Furukawa, S. Goto, T. Mochizuki, T. Uruga, T. Takeshita, T. Ohashi, T. Matsushita, and S. Takahashi, Surf. Rev. Lett. **10**, 501 (2000).

[29]S. Hatta, H. Okuyama, T. Aruga, and O. Sakata, Phys. Rev. B **72**, 081406 (2005).

[30]H.-J. Ernst, E. Hulpke, and J. P. Toennies, Phys. Rev. B **46**, 16081 (1992).

[31]T. Aruga, J. Phys.: Condens. Matter **14**, 8393 (2002).

[32]J. C. Campuzano, M. S. Foster, G. Jennings, R. F. Willis, and W. Unertl, Phys. Rev. Lett. **54**, 2684 (1985).

[33]I. K. Robinson, E. Vlieg, and K. Kern, Phys. Rev. Lett. **63**, 2578 (1989).

[34]L. D. Roelofs, A. R. Kortan, T. L. Einstein, and R. L. Park, Phys. Rev. Lett. **46**, 1465 (1981).

[35]E. Domany, M. Schick, and J. S. Walker, Phys. Rev. Lett. **38**, 1148 (1977).

[36]H. E. Cook, Acta Metall. **23**, 1027 (1975).

[37]H. E. Cook, Acta Metall. **23**, 1041 (1975).

[38]J. A. Krumhansl and J. R. Schrieffer, Phys. Rev. B **11**, 3535 (1975).

[39]M. S. S. Challa, D. P. Landau, and K. Binder, Phys. Rev. B **34**, 1841 (1986).

[40]Y. Imry and J. Scalapino, Phys. Rev. A **9**, 1672 (1974).

[41]L. Petersen, Ismail, and E. W. Plummer, Prog. Surf. Sci. **71**, 1 (2002).

[42]T. C. Chiang, M. Y. Chou, T. Kidd, and T. Miller, J. Phys.: Condens. Matter **14**, R1 (2002).